

Structure of Dayside Polar Cusp Precipitation during the Northward Interplanetary Magnetic Field

V. G. Vorobjev^a, * and O. I. Yagodkina^a

^a Polar Geophysical Institute, Apatity, 184209 Russia

*e-mail: vorobjev@pgia.ru

Received July 29, 2022; revised August 15, 2022; accepted August 22, 2022

Abstract—The unique trajectories of DMSP spacecraft relative to a dayside polar cusp are considered. They allow the cusp precipitation to be characterized in different longitudinal sectors for short time intervals of 2–3 min. The latitudinal widths of a cusp depend on the magnetic local time (MLT) and differ considerably in the pre- and after-noon sectors. A large-scale trend in ion energy fluxes upon a change in MLT can be observed in a cusp, along with smaller variations in energy fluxes having longitudinal dimensions of ~100–150 km. The latitudinal widths of a cusp are determined mainly by the solar wind dynamic pressure (P_{sw}). The width of a cusp is 2.0° – 2.5° of latitude at $P_{sw} = 17$ – 19 nPa and only $\sim 0.3^{\circ}$ at $P_{sw} \approx 1.0$ nPa.

DOI: 10.3103/S1062873822120280

INTRODUCTION

A daytime polar cusp (one in each hemisphere) is a funnel-shaped structure in the geomagnetic field through which solar wind plasma penetrates directly to the ionosphere along lines of the magnetic field. Studying the morphology of cusps and the dynamics and structure of cusp precipitation is an important part of analyzing the interaction between the Earth's magnetosphere and the interplanetary magnetic field (IMF) and solar wind plasma, in addition to how solar plasma penetrates into the magnetosphere.

Comparing satellite observations at different altitudes allows us to characterize particles in different regions of precipitation in the daytime sector and determine the criteria for identifying precipitation in a cusp and adjacent regions from observations of precipitating particles on low-altitude satellites [1]. An automated system for determining the structure of precipitation in the daytime sector based on the data of low-orbiting DMSP satellites was created in [2]. Fast orbits and the presence of several satellites contributed to frequent crossings of the daytime region of precipitation. This helped to accumulate enough observational material to determine the morphological characteristics and dynamics of a polar cusp by the early 1990s.

Statistical studies (e.g., [1–3]) contributed to the development of an averaged cusp model. It was shown that a cusp is a region of $\sim 1^{\circ}$ in latitude and ~ 2.5 h MLT in longitude at ionospheric altitudes. A cusp is roughly symmetrical about its central part, which is usually in the region of the noon meridian and shifts by ~ 1 h MLT toward the pre-noon (afternoon) side at negative (positive) of IMF component B_y in the

Northern Hemisphere. On average, the peak of energy fluxes inside a cusp is closer to its equatorial boundary than to polarward one. The annual average composition of the precipitation spectrograms shows that the properties of a cusp change relatively weakly along with the MLT. This average cusp pattern is supported by patterns of the distribution of precipitation in the daytime sector (e.g., [4]), as has been suggested in a number of works.

The properties of a cusp have been studied in most detail at high and middle altitudes, based on Polar satellite observations [5] and as part of the Cluster project [6]. The statistics of observations at these satellites generally agree with the DMSP results and add some detail. For example, 459 crossings of the cusp region were studied by the Polar satellite in [5]. The average position of a cusp center was shown to be $\sim 80.3^{\circ}$ invariant latitude at noon and shifted $\sim 1.5^{\circ}$ of latitude toward the equator by 08:00 MLT and 16:00 MLT. A cusp structure and dynamics are determined by the IMF parameters and the solar wind dynamic pressure. Observations at different altitudes in a cusp confirm its strong variability. A fast response of a cusp to variations in IMF was noted in [6]: the velocity of convection in the cusp and its configuration changed for just a few minutes.

It is therefore logical to assume that the average statistical characteristics of a cusp considered above are very rarely observed under natural conditions. This is especially true for the longitudinal characteristics of a cusp. During each observation of a cusp, satellites provide information only within a limited MLT region.

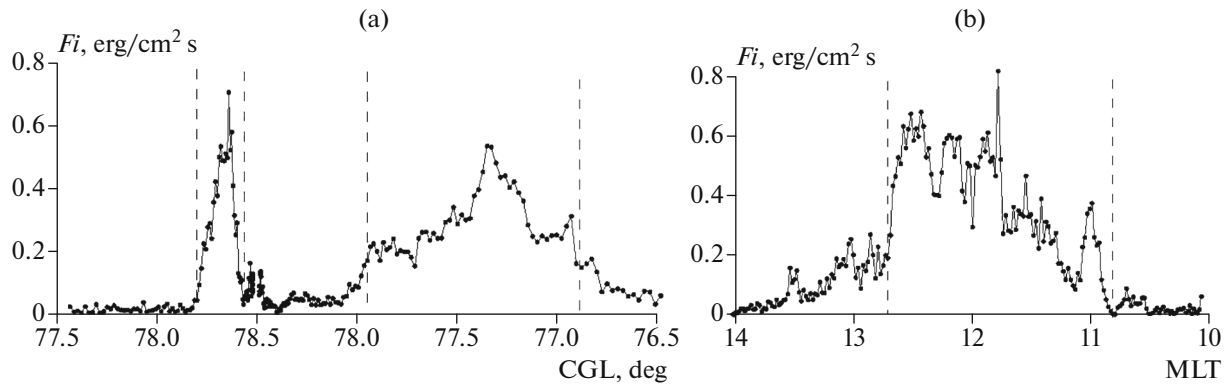


Fig. 1. Cusp observations from satellite F13: variations in the energy fluxes of precipitating ions (F_i , $\text{erg cm}^{-2} \text{s}^{-1}$) at (a) 10:06–10:10 UT on March 18, 2002, and (b) 11:35–11:38 UT on March 19, 2002. The cusp boundaries are marked with vertical dashed lines.

Cusp parameters in other MLT sectors remain unknown during this time.

The aim of this work was to show extremely rare configurations of DMSP satellite trajectories relative to a cusp that allow us to characterize cusp precipitation in different MLT sectors within short time intervals. The latitudinal widths of a cusp are studied with allowance for the parameters of the interplanetary medium. The structure of cusp precipitation is analyzed at extreme values of the solar wind's dynamic pressure in specially selected individual flights.

LONGITUDINAL FEATURES OF PRECIPITATION PARAMETERS

All flights of the DMSP satellites considered in this work were recorded in the Northern Hemisphere at positive B_z and negative B_y components of the IMF. The orbits of the satellites were solar oriented, so the MLT and the angle at which a satellite crossed a daytime cusp depended strongly on the inclination of the geomagnetic dipole to the ecliptic plane, and on the latitude of the cusp region. Two unique flights of satellite F13, the orbital configuration of which relative to a cusp allows us to trace the parameters of precipitation in different MLT sectors over short time intervals, are shown in Fig. 1. The positions of the equatorial and polar boundaries of a cusp are identified according to the criteria in [1] and are shown by the vertical dashed lines. Figure 1a shows variations in the energy flux of precipitating ions (F_i , $\text{erg cm}^{-2} \text{s}^{-1}$) at 10:06–10:10 UT on March 18, 2002. The corrected geomagnetic latitude (CGL) of the satellite's trajectory at an altitude of 110 km is plotted along the abscissa. As the CGL grew, the satellite crossed the cusp in the afternoon sector (i.e., the equatorial boundary at $\sim 78.20^\circ$ CGL and ~ 13.1 MLT, and the polar boundary at $\sim 78.45^\circ$ CGL and ~ 12.6 MLT). Mantle precipitation was recorded at latitudes above the cusp. As the CGL diminished, the satellite crossed the region of

the cusp again, but in the pre-noon sector (i.e., the polar boundary at $\sim 77.95^\circ$ CGL and ~ 11.2 MLT, and the equatorial boundary at $\sim 76.90^\circ$ CGL and ~ 10.40 MLT). The energy flux of precipitating ions was maximal in the cusp, compared the neighboring areas of precipitation (i.e., the mantle poleward of the cusp, and the low-latitude boundary layer (LLBL) equatorward of the cusp). The positions of the F_i maxima in the cusp were recorded at 12.8 MLT and 10.6 MLT with a difference of ~ 2 min between recording times. The energy flux of precipitating ions reached $\sim 0.6 \text{ erg cm}^{-2} \text{ s}^{-1}$ at the maximum and was slightly higher in the afternoon sector than in the pre-noon sector. The approximate latitudinal widths of the cusp were determined from the difference between the latitudes of its polar and equatorial boundaries. The cusp was $\sim 0.25^\circ$ wide in the afternoon sector and much wider ($\sim 1.0^\circ$) in the pre-noon hours of the MLT. The narrow cusp in the afternoon sector was at higher latitudes than even the polar boundary of the cusp in the pre-noon hours. The center of the cusp thus shifted to higher latitudes at an angle of $\sim 10^\circ$ to the geomagnetic parallel from the pre-noon to the afternoon hours.

Figure 1b shows the energy fluxes of precipitating ions from 11:35 to 11:38 UT on March 19, 2002. The satellite coordinate is plotted along the abscissa in MLT. As in the previous flight, the satellite began recording the cusp precipitation in the afternoon sector and stayed inside the cusp for ~ 1.5 min in the 12.7 to 10.8 MLT range of longitudes. Slight changes in the satellite's latitude ($< 0.05^\circ$) at the cusp boundaries give grounds to believe the entire longitudinal range of cusp precipitation was recorded in that flight. At least the cusp width of ~ 2 h MLT can be considered the minimal range of longitudes. Inside the cusp, the satellite latitude varied in the interval of $80.90^\circ \pm 0.15^\circ$ CGL.

As is seen in Fig. 1b, the energy fluxes of precipitating ions changed strongly with MLT. The fluxes were maximal (about $0.65 \text{ erg cm}^{-2} \text{ s}^{-1}$) in the afternoon sector and diminished rapidly by the MLT pre-noon

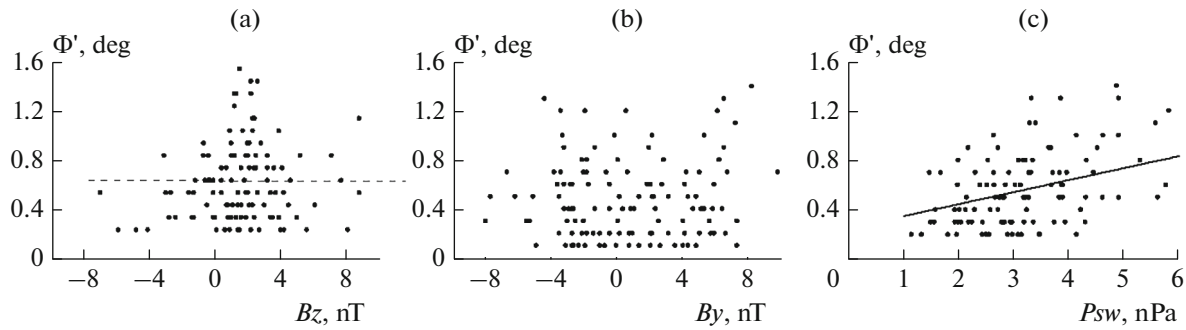


Fig. 2. Latitudinal widths of a cusp ($\Delta\Phi'$) ($^{\circ}$ latitude) versus IMF components (a) B_z and (b) B_y , and (c) the solar wind dynamic pressure.

hours. Wide variations in the energy fluxes with longitudinal dimensions of ~ 100 – 150 km are superimposed by the approximately linear drop in F_i with MLT. The geomagnetic activity was low ($AL > -200$ nT) during the periods of the cusp registration in Fig. 1, and solar wind dynamic pressure P_{sw} was ~ 2.4 nPa.

LATITUDINAL WIDTH OF A CUSP AT EXTREME P_{sw} LEVELS

The latitudinal widths of a cusp vary from a few tenths of a degree to several degrees of latitude. Satellite observations at different altitudes show a slight increase in cusp width with an increase in the solar wind dynamic pressure P_{sw} . Based on statistical material from DMSP observations, a trend toward an increase in cusp width at high absolute values of IMF components B_z and B_y is shown in [7], but the data scatter is considerable. The difficulty is that high values of IMF are usually accompanied by high P_{sw} values. It is impossible to distinguish between the effects different solar wind parameters have on cusp width due to poor statistics for such periods. The Polar and Cluster satellite observations [5, 6] thus showed only that the cusp was somewhat wider at the positive polarity of IMF component B_z than at its negative polarity.

We therefore additionally studied cusp width versus the parameters of the interplanetary medium. We used the 1986 database created in [8] on the basis of satellite F7 data to study the structure of daytime precipitation. We selected satellite flights in which the classic sequence of daytime precipitation regions was recorded as the latitude rose: LLBL–cusp–mantle. Recording regions adjacent to the cusp guaranteed that the satellite crossed the cusp completely, from its equatorial to polar boundaries. Only regions recorded by the satellite longer than four seconds during the flight were considered. A total of 142 intersections of the cusp were detected over the year of observations for which data on the solar wind plasma and IMF were available.

Figures 2a–2c show the latitudinal dimensions of a cusp ($\Delta\Phi'$) versus IMF components B_z and B_y and P_{sw} , respectively. According to Figs. 2a and 2b, there was no relationship between cusp width and the IMF components in our data set. The points in Fig. 2a recall the normal distribution of cusp width about relative average $B_z = -0.5$ nT at average/median cusp width $\langle\Delta\Phi'\rangle = 0.6^{\circ}$. There is no correlation between cusp width and the sign or value of IMF component B_y (Fig. 2b). However, Fig. 2c clearly shows an increase in $\Delta\Phi'$ along with P_{sw} at a considerable data scatter. The solid line in Fig. 2c corresponds to linear regression equation $\Delta\Phi' = 0.25 + 0.10P_{sw}$; coefficient of correlation $r = 0.52$. Figure 2 thus suggests the cusp width was effectively influenced by the solar wind dynamic pressure, but not by the IMF components. This is seen especially for its positive polarity, when the positions of the cusp boundaries do not actually change with the value of the B_z component.

The solar wind dynamic pressure is on average 2–3 nPa, and the range of the most probable variations in P_{sw} is ~ 1 – 6 nPa. Analysis of the characteristics of polar cusp precipitation at extreme values of P_{sw} that go beyond this range is possible only for individual satellite flights specially selected for this purpose. Figures 3a and 3b show the structure of cusp precipitation at extremely high dynamic pressures of 17.5 and 19.0 nPa, respectively. The corrected geomagnetic latitude is plotted along the abscissa. As in Fig. 1, the positions of the cusp boundaries are marked by vertical dashed lines. Figure 3a shows the cusp recorded by satellite F14 at 14:23 UT on March 18, 2002. The cusp width in that flight recorded at a longitude of 11.5 MLT was $\sim 2.4^{\circ}$ in latitude. The energy flux of precipitating ions shows a pronounced maximum at the polar boundary of the cusp, and a less pronounced increase in F_i was observed near its equatorial boundary. Figure 3b shows the cusp crossing by satellite F15 on the same day, but at 16:16 UT. The cusp width in that flight was 2.1° at a longitude of ~ 11.0 MLT. The fluxes of precipitating ions were again maximal at the polar boundary of the cusp, and there was a second maximum of lower amplitude in its equatorial part.

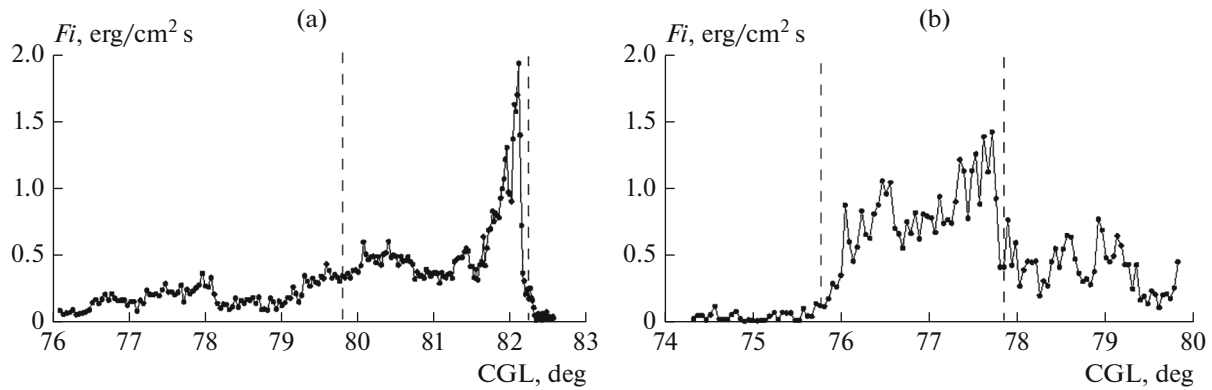


Fig. 3. Structure of cusp precipitation at extremely high solar wind dynamic pressures of (a) 17.5 and (b) 19.0 nPa; energy fluxes of precipitating ions according to the observations of satellites (a) F14 at 14:23 UT and (b) F15 at 16:16 UT on March 18, 2002.

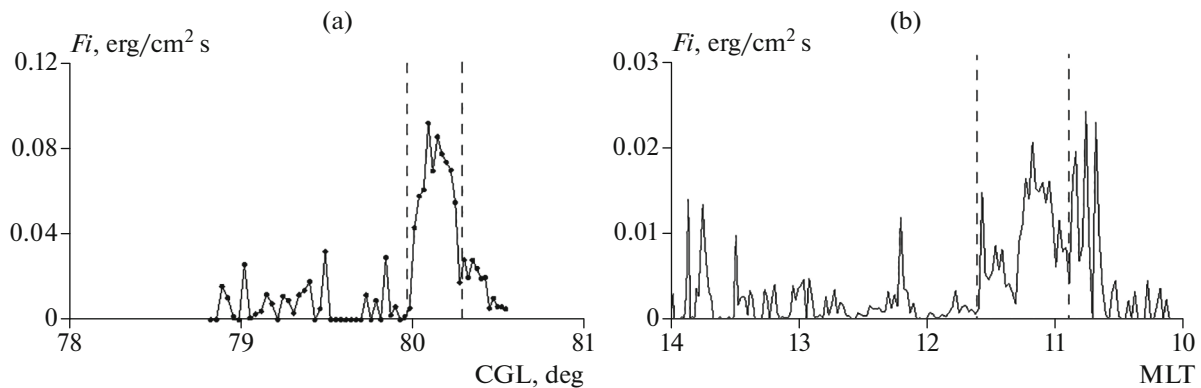


Fig. 4. Energy fluxes of precipitating ions at extremely low P_{sw} values from satellite F18 observations at (a) 13:43–13:45 UT on May 31, 2013, and (b) 11:25–11:28 UT on May 30, 2013.

Figure 4 shows a cusp observed at extremely low P_{sw} . Figure 4a shows a cusp recorded by satellite F18 on the 11.7 MLT meridian at around 13:44 UT on May 31, 2013. The latitudinal widths of the cusp are very small at solar wind dynamic pressure $P_{sw} = 0.87$ nPa and total only 0.3° of latitude. The ion energy fluxes in the cusp are higher than in the regions of precipitation surrounding it, but even the maximum is only $0.1 \text{ erg cm}^{-2} \text{ s}^{-1}$. For comparison, the ion energy fluxes reach $\sim 0.6 \text{ erg cm}^{-2} \text{ s}^{-1}$ at $P_{sw} = 2.4$ nPa in Fig. 1a.

We found no daytime polar cusp records at $P_{sw} < 0.5$ nPa. This could be for two reasons. First, the longitudinal widths of a cusp can be very small during such periods, which greatly lowers the probability of satellites being within the region of cusp precipitation. Second, very low P_{sw} values correspond to weak fluxes of solar wind energy. The criteria for identifying a cusp, derived in [1] for average normal solar wind conditions, can therefore be greatly overestimated, especially in terms of the level of the energy fluxes of precipitating ions. Though extremely rare, small regions of precipitation can be observed in the near-

noon sector. These are similar to cusp precipitation, but with ion energy fluxes below the level determined using criteria from [1]. One such example is shown in Fig. 4b at a solar wind dynamic pressure of 0.27 nPa and IMF components $B_z = 1.5$ nT and $B_y = -1.3$ nT. The MLT of the satellite trajectory is plotted along the abscissa, as in Fig. 1b. The region of precipitation, which is similar to the cusp precipitation recorded by satellite F16 at 11:25–11:28 UT on May 30, 2013, is shown in the figure by the vertical dashed lines. In this region, the average energies of electrons, ions, and electron energy fluxes correspond to the criteria in [1], but the ion energy fluxes are weaker than those normally recorded in a cusp. The size of this cusp-like region is ~ 0.7 h in longitude in 10.9–11.6 MLT, and the maximum energy flux of precipitating ions is $\sim 0.02 \text{ erg cm}^{-2} \text{ s}^{-1}$ —almost an order of magnitude lower than in the event shown in Fig. 4a.

CONCLUSIONS

Data from the DMSP satellites were used to study the structure of ion precipitation in a daytime polar

cusps at a northward oriented IMF component B_z . Unique configurations of the satellite trajectory relative to the cusp were considered, allowing us to determine the characteristics of cusp precipitation in different longitudinal sectors for short time intervals. It was shown that the latitudinal widths of a cusp depend on the MLT and differ considerably in the pre- and afternoon sectors. It was found that a narrow cusp in the afternoon sector was at higher latitudes than even the polarward boundary of the cusp in the pre-noon hours. This indicates a poleward shift of the cusp center at an angle of $\sim 10^\circ$ to the geomagnetic parallel from the pre-noon to the afternoon hours.

Both a large-scale trend of changes in ion energy fluxes with MLT and smaller-scale variations in energy fluxes with longitudinal dimensions of ~ 100 – 150 km can be observed in a cusp. The latter are most likely related to the development of instabilities in the cusp region.

The latitudinal widths of a cusp are mainly determined by the solar wind dynamic pressure. The cusp width is 2.0° – 2.5° latitude at $P_{sw} = 17$ – 19 nPa and only $\sim 0.3^\circ$ at $P_{sw} \approx 1.0$ nPa. High P_{sw} levels were accompanied by high positive values of the B_z component in the events considered in Fig. 3. This produces certain difficulties in distinguishing between the effects of different parameters on the cusp width. However, statistical studies and data on the latitudinal widths of a cusp at extreme P_{sw} levels allow us to conclude that the solar wind dynamic pressure is the main factor of the cusp width in the northward IMF.

The energy flux of precipitating ions shows a pronounced maximum at the polar boundary of a cusp at high P_{sw} . A second, less pronounced peak was observed in energy fluxes near the equatorial boundary of the cusp.

The possible existence of a double maximum in the energy fluxes of precipitating ions during the southward IMF was shown in [7]. A model was proposed in this report that predicted a double maximum during a small southward component B_z and a high azimuthal B_y component of the IMF, based on the theory of magnetic reconnection. The model of a cusp in the northward IMF in [9] revealed no clearly pronounced

double maximum in the ion population. It is possible that the double maximum when $B_z > 0$ can be attributed to extremely high P_{sw} values. During such periods, there can be two sources of cusp ions from high- and low-latitude magnetosheath.

DMSP spacecraft observations revealed no dayside polar cusp at $P_{sw} < 0.5$ nPa. We believe the criteria for cusp identification, derived in [1] for average solar wind conditions, can be strongly overestimated in periods where the solar wind dynamic pressure is extremely low.

The DMSP spacecraft data were taken from <http://sd-www.jhuapl.edu>. Parameters of IMF, solar wind plasma data and indices of magnetic activity came from <http://wdc.kugi.kyoto-u.ac.jp/> and <http://cdaweb.gsfc.nasa.gov/>.

CONFLICT OF INTEREST

The authors declare they have no conflicts of interest.

REFERENCES

1. Newell, P.T. and Meng, C.-I., *J. Geophys. Res.*, 1988, vol. 93, no. A12, 14556.
2. Newell, P.T., Wing, S., Meng, C.-I., and Sigillito, V., *J. Geophys. Res.*, 1991, vol. 96, no. A4, p. 5877.
3. Newell, P.T., Meng, C.-I., Sibeck, D.G., and Lepping, R., *J. Geophys. Res.*, 1989, vol. 94, p. 8921.
4. Newell, P.T. and Meng, C.-I., *J. Geophys. Res.*, 1994, vol. 99, no. A1, p. 273.
5. Zhou, X.W., Russell, C.T., Le, G., Fuselier, S.A., and Scudder, J.D., *J. Geophys. Res.*, 2000, vol. 105, no. A1, p. 245.
6. Pitout, F. and Bogdanova, Y.V., *J. Geophys. Res.*, 2021, vol. 126, no. 9, e2021JA029582.
7. Wing, S., Newell, P.T., and Rouhoniemi, J.M., *J. Geophys. Res.*, 2001, vol. 106, no. A11, 25571.
8. Starkov, G.V., Rezhnev, B.V., Vorobjev, V.G., et al., *Geomagn. Aeron.*, 2002, vol. 42, no. 2, p. 176.
9. Esmaeili, A. and Kalaei, M.J., *Astrophys. Space Sci.*, 2017, vol. 362, p. 124.

Translated by O. Ponomareva